

# Atmospheric stability and wind profile climatology over the North Sea - Case study at Egmond aan Zee

Ameya Sathe  
A.R.Sathe@tudelft.nl  
DUWIND, Technical University Delft  
The Netherlands

## Abstract

The statistics of atmospheric stability and non-dimensional wind profiles are studied using the standard surface-layer theory at Egmond aan Zee in the North Sea. Measurements at 21, 70 and 116 m are used to validate the theoretical profiles. Charnock's relation is used to estimate the sea surface roughness. Bulk Richardson number is used to estimate the Obukhov length. The measured sea water temperature has a positive bias of  $0.82^{\circ}\text{C}$  resulting in the dominance of unstable conditions and a poor agreement of the theoretical wind profiles with the measurements. The conditions at Egmond aan Zee are dominated by unstable and neutral stabilities. The theoretical wind profiles agree very well with the measurements in the unstable and neutral conditions. In stable conditions, the wind profiles are over-predicted significantly as the height increases. The scaling of the wind profile with respect to the boundary layer height is necessary under stable conditions and the addition of another length scale parameter is preferred.

**Keywords:** Atmospheric stability, Obukhov length, Wind profiles, Boundary layer height, Sea surface temperature

## 1 Introduction

This study is important for wind energy applications, since wind profiles have a significant influence on the power production and loads on turbines. The IEC standard [1] suggests the use of either a logarithmic profile without the diabatic correction term or an empirical power law with the power exponent depending on wind speed only, although it also depends on the roughness, height and atmospheric stability condition. [2] demonstrated the importance of using diabatic wind profiles for power production calculations and [3] demonstrated the same for simple load calculations considering only steady winds.

The study of the diabatic wind profile started from the pioneering work on a similarity theory [4] (Monin-Obukhov similarity theory - MOST), where the non-dimensional wind shear depends on atmospheric stability. Atmospheric stability was characterized in the form of a length scale, the Obukhov length, corresponding roughly to the height where the production of the heat and momentum flux are considered to be equal. The advent of MOST led to experimental research

on the empirical similarity relations between the non-dimensional wind shear and atmospheric stability such as those derived from the well-known Kansas experiment [5]. The conditions for which the similarity relations from [5] are derived depict flat and homogeneous terrain satisfying the assumptions of MOST to the best possible extent. Subsequently suggestions to the similarity relations were made [6, 7, 8] which are also used depending on the terrain conditions and the applications.

The applicability of MOST to marine conditions is not obvious as in marine conditions the aerodynamic roughness length varies over the sea. The wind speed dependence on the aerodynamic roughness length over the sea is traditionally represented by the Charnock's relation [9]. Studies have shown its dependence on fetch [10] and wave age [11] as well. Numerous studies of wind profiles have been conducted in the past over the land and sea and a comparison of various corrections to the non-dimensional wind shear due to stability is made in [7]. Experimental verification over the sea is still a challenge. [12] studied the wind profile over

the sea using the data from Sable Island and concluded that the thermal stratification effect is quite significant on wind profiles. [13] studied the diabatic wind profile over the North Sea and found better agreement with the measurements than the neutral logarithmic profile. [14] studied the wind profiles in the Dutch North Sea using measurements (up to 75 m) from various platforms and found that the conditions are mainly unstable and that the surface-layer theory agreed well with the measurements. Recently [15] studied the marine wind profiles with the goal to understand the advection effects (warm air from the land towards sea) on wind profiles and suggested a correction term to be used in the traditional diabatic wind profiles. [16] compared measurements at different offshore sites in the Baltic Sea and verified the validity of the diabatic wind profiles with the measurements. [17] proposed a new model of wind profile for the entire boundary layer based on the assumption that the friction velocity varies linearly with height. With the advent of remote sensing systems the wind profiles were also studied using lidars [18] and a new method was proposed to depict wind profiles in a non-dimensional form [19]. Subsequently a modified wind profile using the theory from [17] is suggested for the marine boundary layer in [20].

The goal of this work is two fold. First is to derive the climatology at Egmond aan Zee in the North Sea in terms of daily, seasonal and overall stability distribution. Second is to investigate the wind profiles using the measurements from the meteorological mast (met-mast). Two mixing-length models of wind profiles are used. The first is the surface-layer wind profile and the second is the extended model of wind profile covering the entire boundary layer from [17].

## 2 Theoretical background

The starting point for wind profile derivation is the assumption that the local wind shear can be derived using Prandtl's mixing length theory,

$$\frac{\partial u}{\partial z} = \frac{u_{*0}}{\kappa l}, \quad (1)$$

where  $u$  is the horizontal wind velocity at a given height  $z$ ,  $u_{*0}$  is the local friction velocity,  $\kappa = 0.4$  is the von Kármán constant and  $l$  is the local length scale. In the surface layer,  $l = z$  and the wind

shear integrates to

$$u = \frac{u_{*0}}{\kappa} \ln\left(\frac{z}{z_0}\right), \quad (2)$$

where  $z_0$  is the aerodynamic roughness length. Over the sea,  $z_0$  can be estimated by the Charnock's relation,

$$z_0 = \alpha \frac{u_{*0}^2}{g}, \quad (3)$$

where  $\alpha$  is the Charnock parameter ( $\alpha = 0.0144$  is used in this analysis based on [21]) and  $g$  is the acceleration due to gravity. Under diabatic conditions the non-dimensional surface-layer wind shear scales with atmospheric stability (according to MOST) as,

$$\frac{\partial u}{\partial z} \frac{\kappa z}{u_{*0}} = \phi_m(z/L), \quad (4)$$

where  $L$  is the Obukhov length given as,

$$L = -\frac{u_{*0}^3 T}{\kappa g w' \theta'_v}. \quad (5)$$

Here  $T$  is the absolute temperature,  $\theta_v$  is the virtual potential temperature and  $\overline{w' \theta'_v}$  is the virtual kinematic heat flux. The form of the  $\phi_m(z/L)$  function has been established under stable and unstable conditions using the Businger equations [5] and the integration of Eq. (4) with the corresponding  $\phi_m$  function gives the diabatic wind profile,

$$u = \frac{u_{*0}}{\kappa} \left[ \ln\left(\frac{z}{z_0}\right) - \psi_m(z/L) \right], \quad (6)$$

where the  $\psi_m$  functions from [5] are used.

[17] extended the wind profile for the entire boundary layer, based on the assumption that the length scale  $l$  in Eq. (1) is an inverse summation of three length scales,

$$\frac{1}{l} = \frac{1}{L_{SL}} + \frac{1}{L_{MBL}} + \frac{1}{L_{UBL}}, \quad (7)$$

where  $L_{SL}$  is the length scale in the surface layer,  $L_{MBL}$  is the length scale of the middle boundary layer and  $L_{UBL}$  is the length scale of the upper boundary layer. The justification of using the inverse summation is not explained in [17] but it could be well explained if we assume that the wind profile in the entire boundary layer is a linear sum of wind profiles in the surface, middle and the upper boundary layer. The derivation of the extended wind profiles is given in [17] and only the final forms are shown here. These are,

$$U = \frac{u_{*0}}{\kappa} \left[ \ln\left(\frac{z}{z_0}\right) + \frac{z}{L_{MBL}} - \frac{z}{z_i} \left( \frac{z}{2L_{MBL}} \right) \right] \quad (8)$$

for neutral conditions,

$$U = \frac{u_{*0}}{\kappa} \left[ \ln \left( \frac{z}{z_0} \right) - \psi_m(z/L) + \frac{z}{L_{MBL}} - \frac{z}{z_i} \left( \frac{z}{2L_{MBL}} \right) \right] \quad (9)$$

for unstable conditions and

$$U = \frac{u_{*0}}{\kappa} \left[ \ln \left( \frac{z}{z_0} \right) - \psi_m(z/L) \left( 1 - \frac{z}{2z_i} \right) + \frac{z}{L_{MBL}} - \frac{z}{z_i} \left( \frac{z}{2L_{MBL}} \right) \right] \quad (10)$$

for stable conditions, where  $z_i$  is the height of the planetary boundary layer.  $z_i$  is assumed to be climatologically proportional to  $u_{*0}$  under neutral conditions as,

$$z_i = c \frac{u_{*0}}{|f_c|}, \quad (11)$$

where  $f_c$  is the Coriolis parameter and  $c$  is a proportionality constant. For a neutral homogeneous terrain, [?] estimated  $c = 0.15$  from the reanalysis of the Leipzig wind profile. Considering that the conditions over the sea are not far from homogeneous, the same value of  $c$  is used in this work. However, under diabatic conditions, there is no agreement on a diagnostic expression for  $z_i$  [22]. In the absence of measurements, it is quite logical to expect that the climatological  $z_i$  decreases as the conditions become more stable. Hence, a decreasing value of  $c$  is applied when the conditions are more stable;  $c = 0.14$  is used for stable conditions and  $c = 0.13$  for very stable conditions (similarly as done in [20]). In accordance with the findings in [?] from the analysis of aerosol profiles, the mean value of  $z_i$  obtained during the neutral conditions is also applied for the unstable conditions.

A new scaling parameter in Eqs. (8–10) is  $L_{MBL}$ . [17] used Rossby number similarity (RST) to equate the geostrophic wind with Eqs. (8–10) at  $z = z_i$ . However, this results in the dependence of  $L_{MBL}$  on the resistance law constants  $A$  and  $B$ , which are uncertain under diabatic conditions, and on the  $\psi_m$  functions, which are unknown up to  $z_i$ .  $L_{MBL}$  can also be fitted to Eqs. (8–10) using measurements and an empirical formulation can be devised [17].

The traditional way of depicting a wind profile is by plotting the non-dimensional wind speed ( $u/u_{*0}$ ) against the non-dimensional height ( $z/z_0$ ). Over sea,  $z_0$  is not a constant and hence the traditional representation is inadequate in a statistical evaluation, since the individual

non-dimensional wind profiles vary with  $z_0$  and  $L$ . Following [19], the neutral wind profiles are depicted in a non-dimensional form as,

$$\frac{u}{u_{*0}} + \frac{1}{\kappa} \ln \left[ 1 + 2 \frac{\Delta u_{*0}}{u_{*0}} + \left( \frac{\Delta u_{*0}}{u_{*0}} \right)^2 \right] = \frac{1}{\kappa} \ln \left( \frac{z}{z_0} \right), \quad (12)$$

where for each stability class,  $\overline{u_{*0}}$  is the mean friction velocity,  $\Delta u_{*0}$  is the fluctuation of the friction velocity and  $\overline{z_0} = \alpha \overline{u_{*0}}^2 / g$  is the mean roughness length. Thus, under neutral conditions, the theoretical non-dimensional profiles match exactly with the non-dimensional height scaled with  $\overline{z_0}$ . Under diabatic conditions the appropriate  $\psi_m$  function is subtracted from the non-dimensional height in Eq. (12). The advantage of this approach is that the wind profiles for a given stability collapse onto a single profile. This approach can be used with the extended wind profiles, Eqs. (8–10), by adding appropriate terms to the non-dimensional height. Thus, the variability of the marine wind profiles can be observed with respect to stability only.

### 3 Dataset

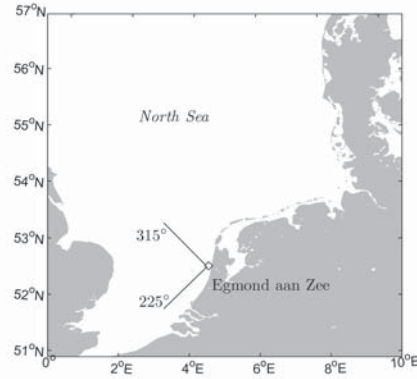


Figure 1: Location of the OWEZ (read Egmond aan Zee) met-mast in the North Sea.

Figure 1 shows the measurements at Egmond aan Zee (henceforth referred to as OWEZ) in the North Sea. The met-mast is located at about 18 km from the coast of Egmond aan Zee, The Netherlands, coordinates  $52^{\circ}36'22.9''$  N,  $4^{\circ}23'22.7''$  E, and is used as the reference for the first Dutch offshore wind farm. The depth of water is approximately 20 m. The sector that is not influenced by the wakes of the turbines is  $135^{\circ}$ – $315^{\circ}$ . The dominant wind direction is

between  $180^\circ$ – $300^\circ$  (see figure 2b). In order to further avoid the coastal effects and the internal boundary layer from the land-sea interaction, the sector that is chosen in this analysis is  $225^\circ$ – $315^\circ$ .

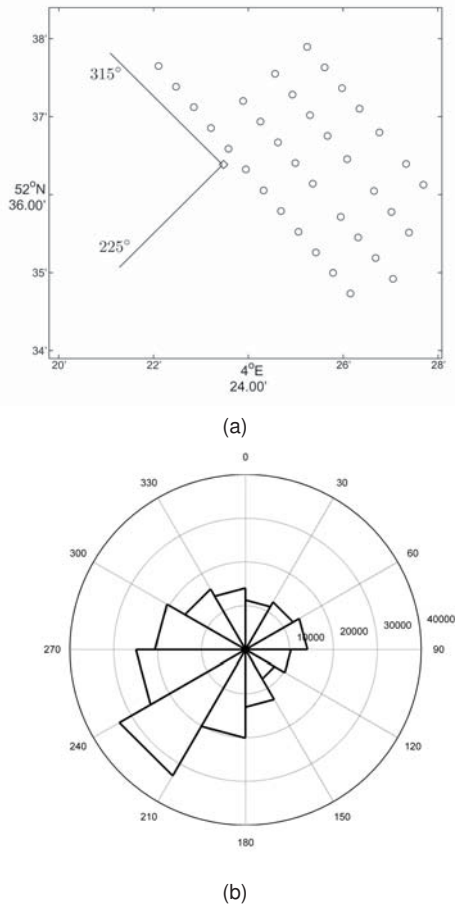


Figure 2: Location of the met-mast with respect to the wind farm (top) and wind rose at 21 m (bottom)

The site comprises 36 Vestas V90 turbines. The measurements are done at three levels, 21, 70 and 116 m. The analysis is carried out using the 10-min mean measurements between July 2005 and December 2009. Mierij Meteo cup anemometers are placed in three directions to avoid direct mast shade on measurements. Wind vanes are also placed in those directions. A combined temperature-humidity sensor is also available at each height. The sea water temperature is measured at 3.8 m below the mean sea level. Ideally the temperature between the air-sea interface is required for the stability analysis to neglect the cool skin and warm layer effects [23]. However, due to lack of sea surface temperatures (SSTs), the sea measurements are considered to repre-

sent SSTs (henceforth the sea water temperature at  $-3.8$  m will be referred as SST). The location of the mast has been chosen such that it ensures the measurement of free stream wind speed from the wind in the dominant South-West direction (see figures 2a and 2b). In order to select a particular cup anemometer and wind vane, preliminary checks are applied to avoid mast effects on measurements (details are given in [24]). Observations of wind speeds greater than 4 m/s are used.

## 4 Results

The results are divided into two categories:

- Statistics of atmospheric stability
- Validation of wind profiles

MOST is based on the assumptions of stationarity and constant fluxes in the surface layer. Non-stationarities in the data are checked following [15]. Usually the height of the surface layer is about 60–100 m during unstable and neutral conditions and less than about 30 m during stable conditions. Preliminary checks revealed that if a filter based on surface-layer height is applied then only 5% of the available measurements are usable. The study of climatology with such limited data is not of much use. Hence, no filter is applied to the data based on the surface-layer height. Seven stabilities are used to classify the observations (see table 1) as given in [17]. [24] attempted to reason the choice of using a

very stable	$10 \leq L \leq 50$ m
stable	$50 \leq L \leq 200$ m
near-neutral stable	$200 \leq L \leq 500$ m
neutral	$ L  \geq 500$ m
near-neutral unstable	$-500 \leq L \leq -200$ m
unstable	$-200 \leq L \leq -100$ m
very unstable	$-100 \leq L \leq -50$ m

Table 1: Classification of atmospheric stability according to Obukhov length intervals

particular classification (e. g. the classification in [14, 16] is different from that in [17]) and concluded that for describing the statistics of atmospheric stability, table 1 is appropriate.

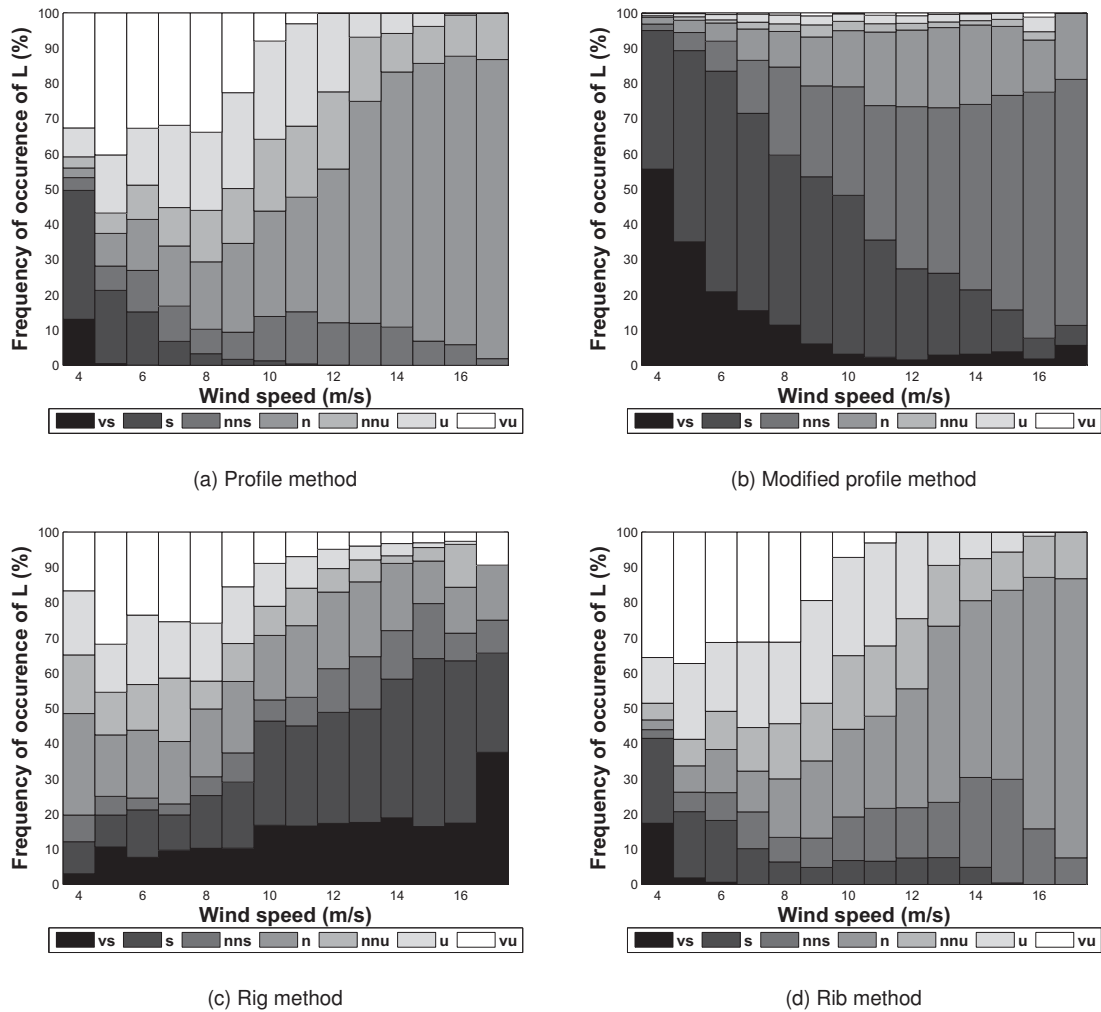


Figure 3: Distribution of  $L$  against different wind speeds using different methods to estimate  $L$

#### 4.1 Performance of different methods to estimate $L$

In the absence of high frequency wind and temperature measurements, 10-min mean measurements can be used to estimate  $L$ . Following methods are compared:

- Profile method [13, 25] - The measurements used are wind speed at 21 m, air temperature at 21 m and SST
- Modified Profile method [16] - The measurements used are wind speed at 21 m, air temperatures at 21 m and 70 m
- Gradient Richardson number (Rig) method [2, 26] - The measurements used are wind speeds at 21 m and 70 m, and air temperatures at 21 m and 70 m

- Bulk Richardson number (Rib) method [27] - The measurements used are wind speed at 21 m, air temperature at 21 m and SST

Figure 3 shows the distribution of  $L$  with wind speeds. The number of neutral conditions increase with wind speed for profile and Rib methods. For the modified profile method there are many stable conditions, whereas for the Rig method the number of stable conditions increase with wind speed. The wind and temperature profiles are assumed to be valid under all conditions for the profile methods. This results in over-prediction of wind profiles under stable conditions [24]. Owing to the higher measuring height (up to 70 m) for the modified profile method, it results in unexpected distribution of  $L$ . For the Rig method it can be shown that  $z/L$ , and therefore  $\psi_m$  function becomes dependent on the inverse of the square of the wind speed difference between the

two levels ( $1/\Delta u^2$ ). The deviation between the measured and predicted profile is therefore enhanced. As expected, the neutral conditions increase with wind speed for the Rib method. It does not require two wind speed measurements to estimate  $L$ . It has also been consistently used in recent studies [2, 19, 20]. Hence, Rib is used to estimate  $L$ .

## 4.2 Statistics of atmospheric stability

The statistics are presented as daily, monthly and overall distributions of  $L$ . For these results the SSTs are corrected by subtracting  $0.82^\circ\text{C}$ . Without this correction, the measured non-dimensional wind profiles have a significant offset compared to the theoretical wind profiles (Eq. 12) under all conditions, even at the lowest measurement height. This offset might be originated from the measurements. A combination of satellite and in-situ measurements from the ERA interim (ECMWF) dataset were used for the comparison with the OWEZ SSTs for a period between July 2005 and October 2008 (see Appendix). It is observed that there is a mean offset of  $0.82^\circ\text{C}$  at OWEZ.

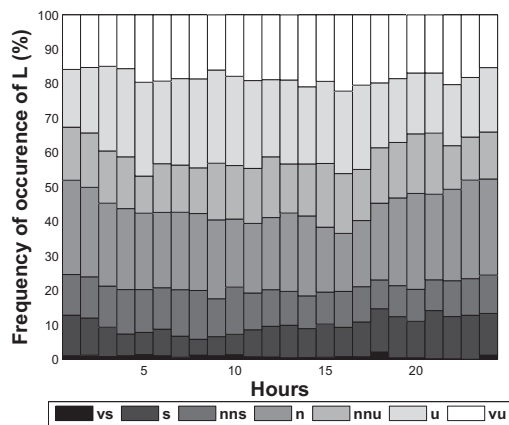


Figure 4: Daily variation of atmospheric stability

Figure 4 shows the daily variation in atmospheric stability, where no significant diurnal variation is observed. There is only a slight increase in the unstable conditions during the day and a slight increase in the stable conditions during the night. The minimum fetch at OWEZ is 160 km from the British coast and there might be little influence from the winds blowing from England.

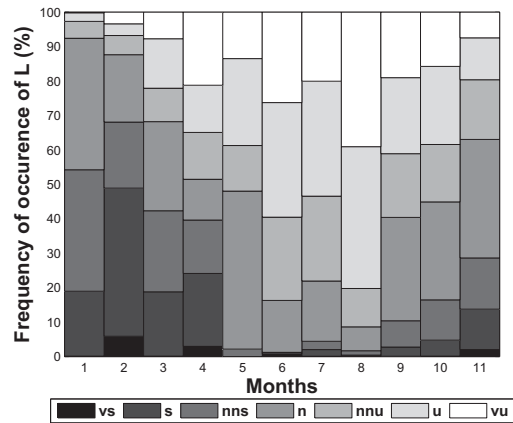


Figure 5: Seasonal variation of atmospheric stability

Figure 5 shows the seasonal variation of atmospheric stability. There is a clear seasonal component of atmospheric stability. The statistics for the month of December are not shown due very limited data. There is, as expected, a marked increase of the unstable conditions during the summer months and an increase of the stable conditions during the winter months. The peak of unstable conditions is found in late summer (August/September) because of the heat capacity of the water, whereas the peak in the stable conditions occur in late winter (February/March).

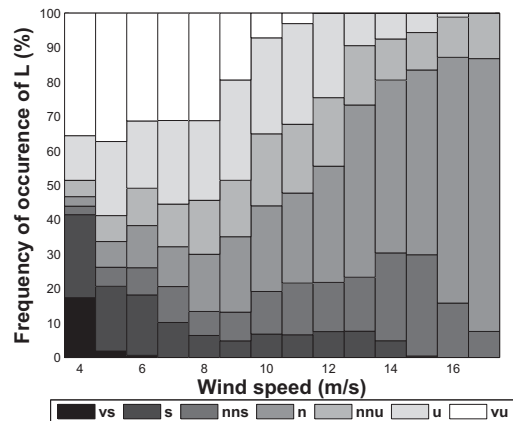


Figure 6: Variation of atmospheric stability with respect to wind speeds

Figure 6 shows the variation of atmospheric stability with wind speed. In general, there is an increase in the neutral conditions with wind

speeds, as expected, since momentum flux dominates over the heat flux at high wind speeds. There is a slight increase in the near-neutral stable conditions at certain wind speeds – 14 and 15 m/s. There are many values of  $L$  within the range of 400–500 m, where the spikes are observed. Lowering of the threshold (from 500 to 400 m, table 1) for the neutral interval results in a substantial increase in the number of neutral conditions for those wind speeds and no spikes are observed any longer. Stability classification is rather sensitive to those values of  $L$  which are in the edges of the interval. Considering the uncertainty in the estimation of  $L$ , these spikes are not significant.

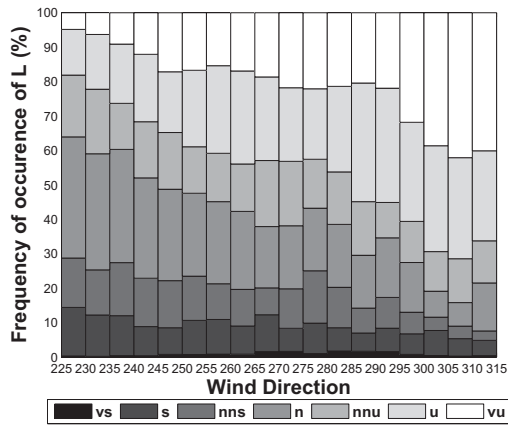


Figure 7: Variation of atmospheric stability with wind direction

Figure 7 shows the variation of atmospheric stability with wind direction. A systematic increase in the number of unstable conditions is observed as the wind direction changes from South-West to North-West, where there is a large open fetch (see figure 1). In the South-West direction wind is affected by the British Coast whereas in the North-West direction the wind essentially comes from the sea. The number of stable conditions reduce towards the North-West direction because of the cold winds over warmer sea that produce unstable condition. This is in agreement with the findings in European wind Atlas [28], where it was concluded that on a climatological average, land conditions in Europe are stable and sea conditions are unstable.

Figure 8 shows the overall distribution of atmospheric stability. In general the conditions are mainly neutral and unstable in agreement with the climatological findings in [28]. This is also in con-

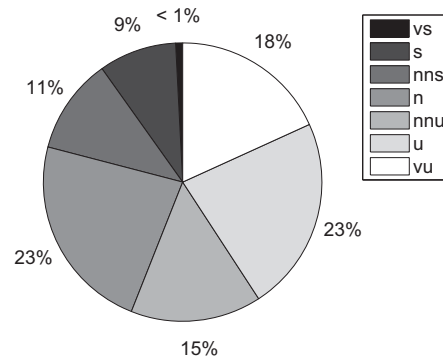


Figure 8: Overall distribution of atmospheric stability

formity with the observations in [14], where the study was carried out in the Dutch part of the North Sea.

### 4.3 Non-dimensional wind profiles

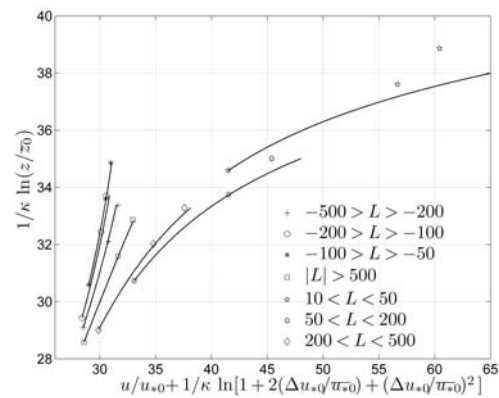


Figure 9: Non-dimensional wind profiles in the North Sea. Measurements are shown by different markers

Figure 9 shows the non-dimensional wind profile at OWEZ. The measurements are divided into seven stability classes (table 1) and a mean (theoretical and measured) profile is plotted for each stability class. The mean observed parameters are given in table 2.

The theoretical profiles are estimated using Eq. (12). They agree very well with the measurements in unstable and neutral conditions. This result is quite significant since there is ongoing

$L$ (m)	$u_{*0}$ (m/s)	No. of Profiles
-74	0.26	3959
-140	0.33	4913
-311	0.36	3303
$ L  = 4999$	0.39	5013
321	0.36	2416
128	0.26	1960
41	0.12	133

Table 2: Mean observed parameters in each stability class used for plotting the wind profiles according to Eqs. (6) and (12)

debate on the use of diabatic wind profiles (Eq. 6) in wind energy. A recent study [20] has indicated (using different dataset) that Eq. (6) can be used for the unstable and neutral conditions even beyond the surface layer and the wind profiles at OWEZ (figure 9) conform with these findings.

For stable conditions, the wind profiles are over-predicted significantly with increasing height. Due to the linear dependence of the non-dimensional wind shear with the stability parameter ( $z/L$ ), at greater heights such an over-prediction is quite expected. Scaling with  $z_i$  tends to reduce the wind shear at greater heights considerably [20]. In the model of [17] there is additional dependence of wind speed profile on  $z_i$  and  $L_{MBL}$ . [20] argued that  $L_{MBL}$  over the sea is quite large ( $L_{MBL} \gg z$ ), and hence, its influence can be neglected. This results in scaling the wind profile under stable conditions with  $z_i$  only and the wind profiles for the unstable and neutral conditions converge with those in the surface layer (Eq. 6). In this work, as a preliminary study,  $L_{MBL}$  was fitted to the OWEZ measurements according to Eqs. (8–10). It was found that  $L_{MBL}$  is very large for unstable and neutral conditions in accordance with [20], whereas for stable conditions  $L_{MBL}$  could not be neglected. [17] further showed that  $L_{MBL}$  depends on the resistance law constants  $A$  and  $B$ . In this analysis the values for  $A$  and  $B$  from [?] were used (despite the fact that considerable scatter is observed under diabatic conditions) to estimate the influence of  $L_{MBL}$  on the wind profiles in conjunction with  $z_i$ . The  $A$ ,  $B$ ,  $z_i$  and  $L_{MBL}$  values used to obtain the extended wind profiles for stable conditions (Eq. 10) are given in Table 3.

Figure 10 shows the extended wind profiles using Eqs. (10) and (12), and neglecting the effect of  $L_{MBL}$ . It is observed that the theoretical profile

$L$ (m)	321	128	41
$A$	1.5	1.5	1.6
$B$	5.2	5.2	5.2
$z_i$ (m)	205	117	49
$L_{MBL}$ (m)	866	283	69

Table 3: Mean parameters used for the stable wind profiles according to Eqs. (10) and (12)

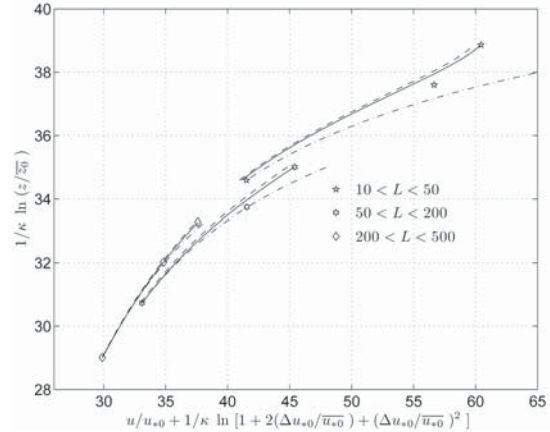


Figure 10: Extended wind profiles at OWEZ showing the influence of  $z_i$  and  $L_{MBL}$  under stable conditions. The dashed line shows the influence of  $z_i$  only and the solid line shows the combined effect of  $z_i$  and  $L_{MBL}$ . The dash-dot line shows the traditional surface-layer theory

has a slightly better agreement when the combined effect of  $z_i$  and  $L_{MBL}$  is considered than assuming only the effect of  $z_i$ . Both approaches agree better with the observations than surface-layer theory. The influence of the approach of using  $z_i$  only is to slightly under-predict the wind profile.

## 5 Discussion and Conclusion

Atmospheric stability and wind profile climatology is studied at OWEZ in the North Sea. It is observed that atmospheric stability is dominated by unstable and neutral conditions due to cold air over warmer sea. Very stable conditions occur rarely. This result is in agreement with the previous analysis by [14], where the study was carried out in the Dutch part of the North Sea. It would be interesting to perform a stability analysis at different latitudes in the North Sea to obtain a spatial the distribution of diabatic conditions.

There is little daily variation of diabatic conditions, characteristic of land conditions. The heat capacity of water causes mainly a seasonal variation. The analysis of the variation of atmospheric stability with wind speed shows a marked increase in the neutral conditions. The amount of observations in the stability classes is dependent on the interval limits.

A different classification has also been suggested previously [14, 16] and its use would increase the number of stable conditions considerably. In the future it would be interesting to arrive to a firm criterion to classify  $L$ . Currently the criterion for selecting the intervals of  $L$  is based only on previous research experience. A systematic increase of unstable conditions from the South-West to the North-West direction at both sites is in agreement with the European wind and stability climatology in [28].

Non-dimensional wind profiles are also studied and the measurements agree very well with the surface-layer theory in unstable and neutral conditions. For stable conditions, surface-layer theory over-predicts the wind speed with increasing heights. In order to assess the influence of  $z_i$  on the the wind profile the theory from [17] is used at OWEZ. This introduces a new parameter,  $L_{MBL}$ . The comparison with the observations of the theoretical profiles at OWEZ, scaled with only  $z_i$  and a combination of  $z_i$  and  $L_{MBL}$  shows better agreement than that of traditional surface-layer theory.

In the North Sea, the description of the wind profiles using the standard surface-layer theory and Charnock's model for  $z_0$  is sufficient for the unstable and neutral conditions. Under stable conditions the wind profiles should definitely be scaled by  $z_i$  and preferably  $L_{MBL}$  should be applied as another scaling parameter. This analysis will aid the wind farm developers to estimate the power production of wind turbines. The influence on the loads of the wind turbines is still a research question.

#### Acknowledgements

The data from the Offshore Wind farm Egmond aan Zee (OWEZ) were kindly made available by NoordZeewind as part of the PhD project under the Research Program WE@Sea. I express my sincere thanks to Sven-Erik Gryning and Alfredo Peña from Risø DTU for guiding me in this work when I was stuck with the poor fit between the theoretical profiles and

measurements. Their idea of using the ECMWF satellite measurements and comparing the horizontal wind speed spectra at two sites added a lot of weight to the justification of modifying the SST. I also thank Wim Bierbooms for supervising my PhD.

## References

- [1] IEC. IEC 61400-1. Wind turbines – Design Requirements. 2005.
- [2] B. Lange, S. Larsen, J. Højstrup, and R. Barthelmie. Importance of thermal effects and sea surface roughness for offshore wind resource assessment. *Journal of Wind Engineering and Industrial Aerodynamics*, 92(11):959–988, 2004.
- [3] A. Sathe and W. Bierbooms. The influence of different wind profiles due to varying atmospheric stability on the fatigue life of wind turbines. In M O L. Hansen and K S. Hansen, editors, *The Science of Making Torque from Wind*, volume 75 of *Journal of Physics: Conference Series*, 2007.
- [4] A S. Monin and A M. Obukhov. Basic laws of turbulent mixing in the atmosphere near the ground. *Tr. Akad. Nauk. SSR, Geofiz. Inst.*, 151:163–187, 1954.
- [5] J A. Businger, J C. Wyngaard, Y Izumi, and E F Bradley. Flux-profile relationships in the atmospheric surface layer. *Journal of the Atmospheric Sciences*, 28:181–189, 1971.
- [6] A J. Dyer. A review of flux-profile relationships. *Boundary-Layer Meteorology*, 7:363–372, 1974.
- [7] U. Höglström. Nondimensional wind and temperature profiles in the atmospheric surface layer. *Boundary-Layer Meteorology*, 42:55–78, 1988.
- [8] A A. Grachev, C W. Fairall, and E F. Bradley. Convective profile constants revisited. *Boundary-Layer Meteorology*, 94(3):495–515, 2000.
- [9] H. Charnock. Wind stress over a water surface. *Quarterly Journal of Royal Meteorological Society*, 81(350):639–640, 1955.
- [10] K K. Kahma and C J. Calkoen. Reconciling discrepancies in the observed growth of wind-generated waves. *Journal of Physical Oceanography*, 22(12):1389–1405, 1992.
- [11] H K. Johnson, J. Højstrup, H J. Vested, and S E. Larsen. On the dependence of sea surface roughness on wind waves. *Journal of Physical Oceanography*, 28(9):1702–1716, 1998.
- [12] J L. Walmsley. On the theoretical wind-speed and temperature profiles over the sea with applications to data from sable-island, nova-scotia. *Atmosphere-Ocean*, 26(2):203–233, 1988.
- [13] A J M. Van Wijk, A C M. Beljaars, A A M. Holtslag, and W C. Turkenburg. Evaluation of stability corrections in wind speed profiles over the North Sea. *Journal of Wind Engineering and Industrial Aerodynamics*, pages 551–566, 1990.

- [14] J P. Coelingh, A J M. van Wijk, and A A M. Holtslag. Analysis of the wind speed observations over the North Sea. *Journal of Wind Engineering and Industrial Aerodynamics*, 61:51–69, 1996.
- [15] B. Lange, S. Larsen, J. Højstrup, and R. Barthelmie. The influence of thermal effects on the wind speed profile of the coastal marine boundary layer. *Boundary-Layer Meteorology*, pages 587–617, 2004.
- [16] M. Motta and R J. Barthelmie. The influence of non-logarithmic wind speed profiles on potential power output at Danish offshore sites. *Wind Energy*, pages 219–236, 2005.
- [17] S-E. Gryning, E. Batchvarova, B. Brümmer, H. Jørgensen, and S. Larsen. On the extension of the wind profile over homogeneous terrain beyond the surface layer. *Boundary layer meteorology*, 124(2):251–268, 2007.
- [18] A. Peña, C B. Hasager, S-E. Gryning, M. Courtney, I. Antoniou, and T. Mikkelsen. Offshore wind profiling using light detection and ranging measurements. *Wind Energy*, 12(2):105–124, 2009.
- [19] A. Peña and S-E. Gryning. Charnock’s roughness length model and non-dimensional wind profiles over the sea. *Boundary-Layer Meteorology*, 128:191–203, 2008.
- [20] A. Peña, S-E. Gryning, and C B. Hasager. Measurement and modelling of the wind speed profile in the marine atmospheric boundary layer. *Boundary-Layer Meteorology*, 129(3):479–495, 2008.
- [21] J R. Garratt. Review of drag coefficients over oceans and continents. *Monthly Weather Review*, 105(7):915929, 1977.
- [22] P. Seibert, F. Beyrich, S-E. Gryning, S. Joffre, A. Rasmussen, and P. Tercier. Review and inter-comparison of operational methods for the determination of the mixing height. *Atmospheric Environment*, 34(7):1001–1027, 2000.
- [23] C W. Fairall, E F. Bradley, J S. Godfrey, G A. Wick, J B. Edson, and G S. Young. Cool skin and warm layer effects on sea surface temperature. *Journal of Geophysical research*, 101:1295–1308, 1996.
- [24] A. Sathe. Project site data - OWEZ data analysis. We@sea report, Technical University Delft, 2009.
- [25] A A M. Holtslag. Estimates of diabatic wind speed profiles from near-surface observations. *Boundary-Layer Meteorology*, 29:225–250, 1984.
- [26] M. Mohan and T.A. Siddiqui. Analysis of various schemes for the estimation of atmospheric stability classification. *Atmospheric Environment*, 32:37753781, 1994.
- [27] A A. Grachev and C W. Fairall. Dependence of the Monin-Obukhov stability parameter on the bulk Richardson number over the ocean. *Journal of Applied Meteorology*, 36:406–414, 1996.
- [28] I B. Troen and E. Petersen. European wind atlas. Technical report, Risø National Laboratory, 1989.
- [29] IFS Documentation Cy33r1. Part ii: Data assimilation. Technical report, ECMWF, 2008.

#### Appendix - Comparison of OWEZ and ECMWF SST

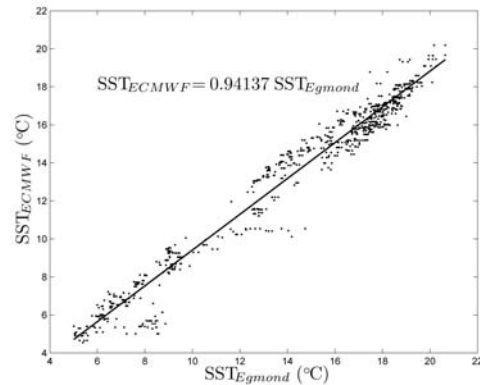


Figure 11: Scatter plot of ECMWF and OWEZ SST

Figures 11 and 12 show the comparison between OWEZ and ECMWF SST. ECMWF SST refers to the foundation temperature which is free of any diurnal variation [29]. The foundation depth varies depending on the state of the atmosphere but is typically larger than 4 m below the sea level. Usually diurnal variations are observed in the first couple of meters below the sea surface. Considering that OWEZ SST refers to measurement at 3.8 m below the sea surface, the SST at OWEZ should not be influenced by diurnal variation. Thus the comparison of the ECMWF and OWEZ SST should not have significant differences. A clear positive bias is observed in the OWEZ SST suggesting that the OWEZ SST should be subtracted by  $0.82^{\circ}\text{C}$  (figure 12 top). As expected the seasonality in the SST is also observed using both datasets (figure 12 bottom).

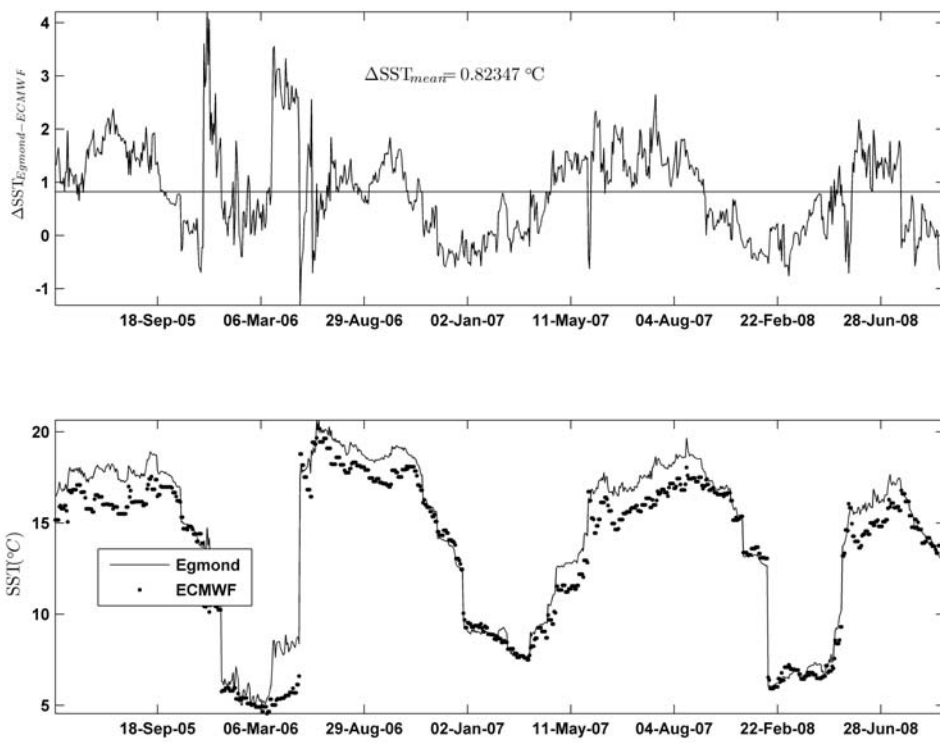


Figure 12: Time series of ECMWF and OWEZ SST